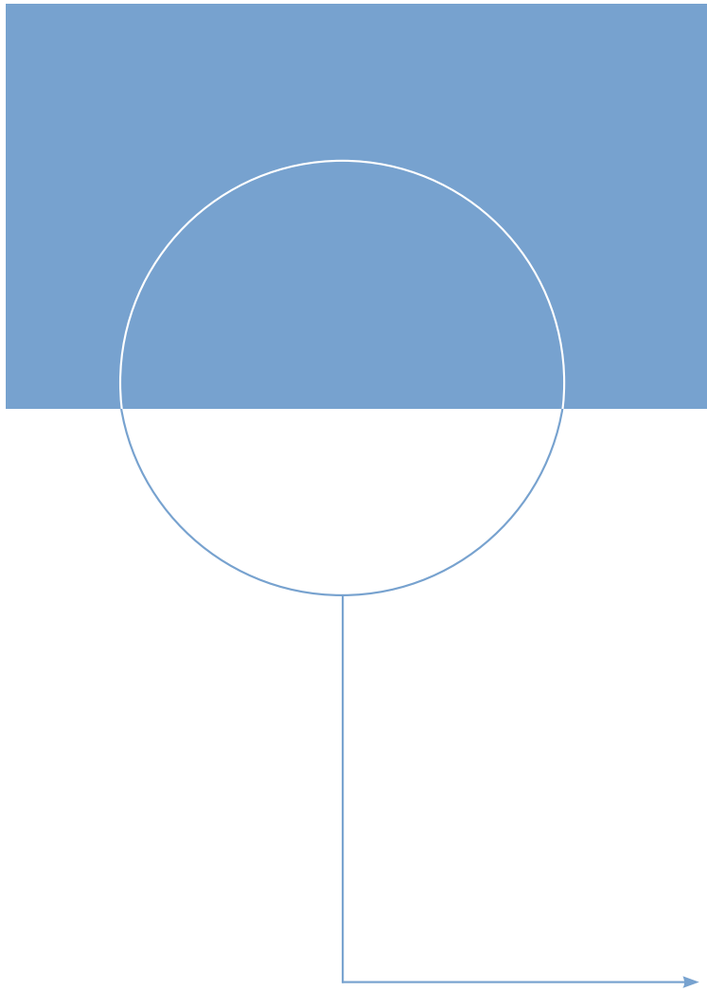

Master's thesis

2021

Eirik Sørmo

**NTNU**
Norwegian University of
Science and Technology
Faculty of Natural Sciences
Department of Chemical Engineering

Eirik Sørmo

# Fluoride Quantification and Removal from Industrial Process Streams

July 2021

NTNU
Norwegian University of
Science and Technology

NTNU
Norwegian University of
Science and Technology

NTNU
Norwegian University of
Science and Technology

# Fluoride Quantification and Removal from Industrial Process Streams

Eirik Sørmo

Chemical Engineering
Submission date: July 2021
Supervisor: Sulalit Bandyopadhyay
Co-supervisor: Seniz Ucar

Norwegian University of Science and Technology
Department of Chemical Engineering

**Abstract**

Iron oxyhydroxides have been precipitated in the presence of fluoride using a Mixed-Suspension-Mixed-Product-Removal(MSMPR) Reactor at different temperatures, residence times and concentrations of sulphate. The levels of temperature used were 25°C and 60°C, the levels of residence time were 30 min and 45 min, while the sulphate concentrations were 0, 10 and 20 g/L. The effect these parameters had on the precipitate and fluoride adsorption were studied.

The crystallinity of the precipitate decreased with decreasing temperature and increasing sulphate concentration. The precipitates without sulphate were 70-80 % akaganeite, while at a sulphate concentration of 20 g/L, the precipitate were only a few per cent akaganeite, while it had a high percentage of schwertmannite.

The concentration of fluoride in the flows entering the reactor where 100 mg/L. The amount left in the filtrate varied between 1.59 mg/L at a temperature of 60°C, residence time of 30 min and no sulphate, to 33.43 mg/L at a temperature of 25°C, residence time of 45 min and 20 g/L of sulphate. It was determined that the main effect of temperature and sulphate concentration were significant, and that they had a significant interaction.

## Acknowledgements

I would like to thank my supervisor Dr. Sulalit Bandyopadhyay and co-supervisor Dr. Seniz Ucar for all the encouragement and help they have provided.

I would also like to thank PhD-student Ina Beate Jenssen for her invaluable support in setting up the reactor and making the software work.

My thanks also go to Dr. Oluf Bøckman at Glencore Nikkelverk AS for sharing his insight into their processes.

# Contents



# List of Figures

# List of Tables

# 1 Introduction

Fluoride is one of the most abundant elements in the earth's crust and sea, estimated to be the 13th most abundant[1]. Humans primarily get fluoride from the water and food we consume, but also in some cases through the air we breathe. Although low doses of fluoride are beneficial for dental health, high levels of fluoride pose a health threat to humans, causing dental and skeletal fluorosis if consumed in high doses. Because of this, the WHO has advised a maximum of 1.5mg/l [2] in drinking water, and the European Union have a maximum advised safe consumption of 7 mg/day [3].

Due to the problems caused by high levels of fluoride, there has been significant work on how to remove it, both from drinking water and industrial waste[4], using methods like precipitation of $CaF_2$ [5–7], adsorption on activated alumina[8], loaded natural zeolite[9], FeOOH[10] and granular ferric hydroxide[11, 12].

The ore that is used in the hydrometallurgical production of nickel contained both undesirable iron and fluoride, and when more of the good quality nickel ore has been used, the amounts of undesirable elements will increase. At Glencore Nikkelverk AS in Kristiansand, Norway, the iron is precipitated in the form of akaganeite and removed through filtration early in the process. Despite that previous work have looked at the adsorption ability[11–15] and precipitation of iron oxide-hydroxide[15–17] separately, little work has been done looking at the adsorption ability of akaganeite during its precipitation and whether the fluoride is integrated into the crystal structure or if it is adsorbed onto the surface, a matter that is of importance in regard of storing the waste.

This thesis will look at this by using a mixed-suspension-mixed-product-removal (MSMPR) reactor at variating temperatures, residence times and concentrations of nickel-sulphate and study the effect this has on the structure and phases of the precipitate and its impact on the removal of fluoride, in addition to determining the location of the fluoride.

# 2 Theory & Literature Review

This chapter will present the theory for precipitation of akaganeite and similar iron hydroxides, and the ability for them to remove fluoride. In addition it will discuss some relevant general theory for precipitation, and the crystal structure of akaganeite.

## 2.1 Akaganeite

Akaganeite is a stable ferric oxide-hydroxide with the chemical formula $FeO_{0.833}(OH)_{1.167}Cl_{0.167}$. The chloride is required to stabilise the structure and is located inside of the tunnels of the akaganeite crystal structure, as shown in Figure 2.1[18]. Although akaganeite normally have chloride inside of the tunnels, it can be exchanged with a suitable ion, fluoride, bromide and hydroxide, or be precipitated without a chloride presence given the presence of a suitable ion to take its place, like fluoride[14, 15]. The possibility of fluoride to take the place of chloride might be explained by them both being halogens, having a charge of -1 and the fluoride having a small enough size, 1.33 Å, compared to chloride, 1.81 Å[19].

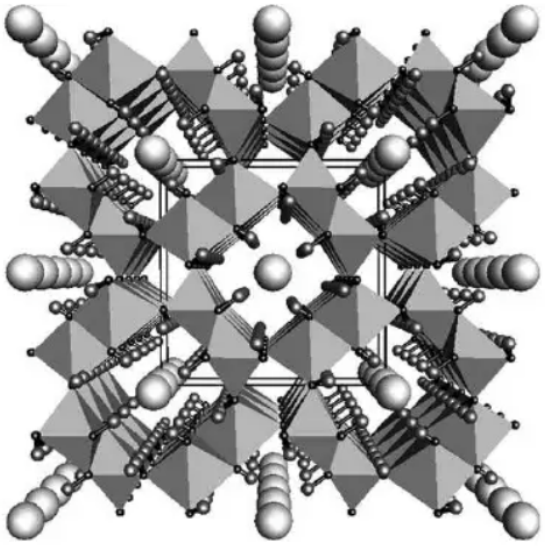

Figure 2.1: Crystal structure of akaganeite[18]

The cell parameters of Cl-akaganeite that had been synthesised from iron(III) perchlorate and NaCl are shown in Figure 2.2. The other cell parameters are from akaganeite that had been incubated in solutions containing the mentioned ions, or pure water for $H_2O$-akaganeite. It shows how the parameters are affected by the ions that occupy the sites in the tunnel.[14]

| sample | *a*, Å | *b*, Å | *c*, Å | 110 position, Å |
|---|---|---|---|---|
| Cl-akaganeite | 10.548 ± 0.001 | 3.030 ± 0.001 | 10.529 ± 0.001 | 7.47 |
| $H_2O$-akaganeite | 10.525 ± 0.001 | 3.031 ± 0.001 | 10.538 ± 0.001 | 7.45 |
| $SO_4$-akaganeite | 10.537 ± 0.001 | 3.030 ± 0.002 | 10.510 ± 0.001 | 7.40 |
| F-akaganeite | 10.481 ± 0.002 | 3.032 ± 0.002 | 10.495 ± 0.002 | 7.35 |
| OH-akaganeite | 10.481 ± 0.002 | 3.029 ± 0.002 | 10.445 ± 0.002 | 7.36 |
| $F/SO_4$-akaganeite | 10.512 ± 0.001 | 3.031 ± 0.001 | 10.485 ± 0.001 | 7.37 |

Figure 2.2: Cell parameters for akaganeite and ion-exchanged akaganeite[14]

## 2.2 Precipitation

Precipitation requires that the solution is adequately supersaturated. Figure 2.3 shows a diagram over the different levels of saturation. The solid line marks the solubility curve, while the dotted line is the super-solubility. In the stable zone, below the solubility line, the solution is unsaturated, and there will be neither nucleation nor crystal growth. In the metastable zone, between the supersolubility and solubility line, the solution is supersaturated and existing crystals may grow, but nucleation is unlikely. The last zone is the labile zone, over the supersolubility line, the solution is supersaturated to such an extent that nucleation can occur, although it may take considerable time. It is possible to make a solution go from the stable zone to the metastable or the labile zone by altering the temperature, normally decreasing it, or increasing the concentration, either by increasing the amounts of ions or decreasing the amount of solvent. Once the supersaturation is in the labile zone, nucleation becomes probable, it may begin spontaneously or be induced by seeding or agitation, and nuclei will begin to form with time. The higher the supersaturation, the faster this nucleation will be, and therefore a higher amount of nuclei will form. With the formation of nuclei, the supersaturation will decrease until it reaches the supersolubility line, when the growth of the nuclei will begin to dominate the crystallisation and nucleation starts becoming rarer and rarer. Because of this, the control of the concentrations and temperature is vital to control the quality of the precipitate. [20]

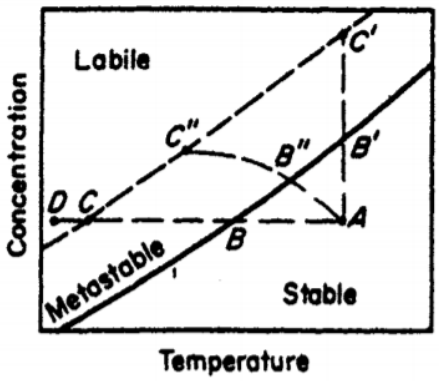


Figure 2.3: Solubility-supersolubility diagram[20]

Figure 2.4 shows that the nucleus formed during the nucleation have a critical size, if it it smaller than this, it will dissolve, if it is bigger, it will persist and grow. The reason for this is that everything will seek to reduce the free energy, and for the growth of crystal there are a competition between the $\Delta G_S$, which is the surface excess free energy and the $\Delta G_V$, which is the volume excess free energy. For the nucleus to be stable it is required that $\Delta G_S + \Delta G_V < 0$. However because the $\Delta G_V$ depends on temperature the critical size of the nucleus will vary depending on the temperature. This is shown in Figure 2.5, where $T_2 > T_1$.[20]

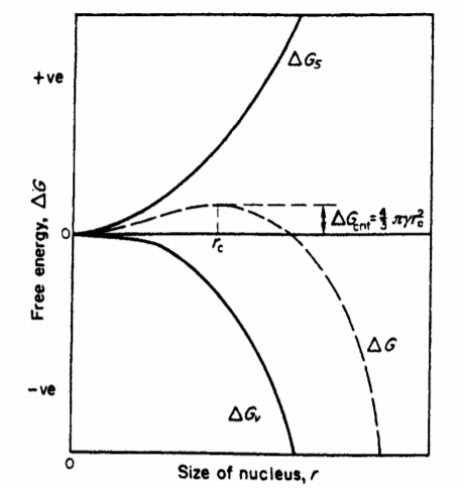


Figure 2.4: Critical nucleus radius[20]

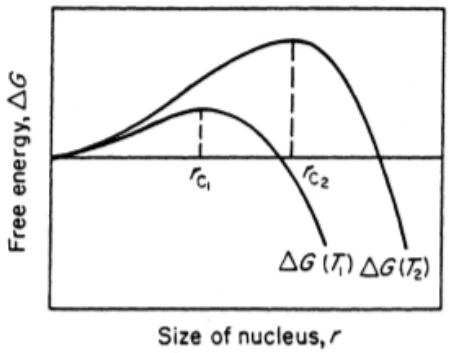


Figure 2.5: Critical nucleus radius dependency on temperature[20]

The formed crystal is not always the ones that are the most stable, it quite common for it to be metastable. The first formed crystal is often the one that is closest to resembling the unstable system. Over time it will however transform into a more stable crystal, although the time required varies. Changes in the condition can alter which crystal is the most stable and the end product. [20]

### 2.2.1 Precipitation of Akaganeite

The precipitation of akaganeite requires a low pH and the presence of either chloride or fluoride to stabilise the tunnels. (Cai, et al. 2001)[15] synthesised akaganeite from $FeCl_3$ to get Cl-akaganeite and from $FeF_3$ to get F-akaganeite. The Cl-akaganeite were prepared at varying pH values and the XRD of them are shown in Figure 2.6. The XRD at pH of 1.5 shows a quite crystalline precipitate of akaganeite, as the pH increases, the akaganeite starts becoming less crystalline and at pH of 6 the precipitate has become hematite and goethite rather than akaganeite. When the pH is increased further, the precipitate is only hematite. These figures show the need for the reaction to have a low pH and how the precipitation of iron hydroxides are affected by pH. [15]

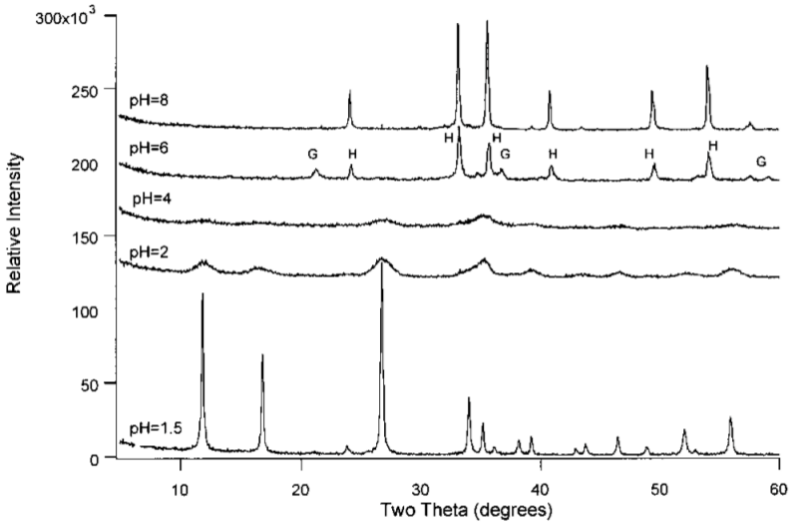


Figure 2.6: XRD of akaganeite prepared from $FeCl_3$ at different pH values. H:hematite; G:goethite [15]

(Peretyazhko, et al. 2018)[17] looks at how pH and initial concentration of chloride affects the product precipitated. The akaganeite were synthesised using Fe(III) perchlorate in the presence of varying concentrations of chloride and initial pH values. The characterisation of the precipitate is shown Figure 2.7 and the Rietveld refinement of the XRD are shown in Figure 2.8. The Rietveld refinement shows how both the pH and the concentration of chloride affect how much of each phase is precipitated. It shows that at the lowest pH of 1.6 and the highest chloride concentration of 0.1M all the precipitate were akaganeite, but with decreasing chloride concentration, the amount of akaganeite decreases. It shows the same tendencies when the pH is increased, but even at a pH of 8 some of the precipitate were akaganeite as long as the chloride concentration were adequately high. This paper shows how both the pH and chloride concentration has a significant impact on the precipitation of akaganeite. The XRD shows how the crystallinity is affected by the changing

conditions. Like in Figure 2.6 the precipitated akaganeite is more crystalline at lower pH values and higher chloride concentrations. [17]

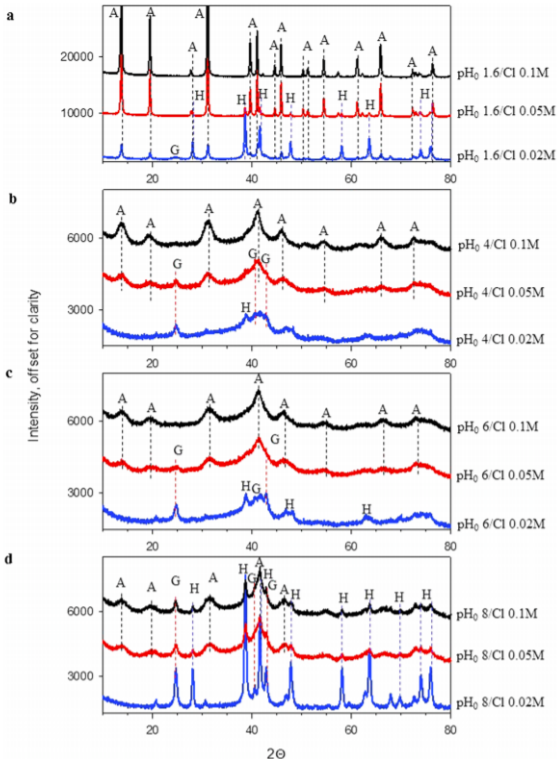


Figure 2.7: XRD of precipitate with variating concentrations of chloride. (a) $pH_0$ 1.6, (b) $pH_0$ 4, (c) $pH_0$ 6, and (d) $pH_0$ 8. A:akaganeite; H:hematite; G:goethite.[17]

| | Fe(III) (hydr)oxide, wt % | | | |
|---|---|---|---|---|
| Sample | Akaganeite | Goethite | Hematite | Ferrihydrite |
| $pH_0$ 1.6/Cl 0.1 M | 100 | 0 | 0 | 0 |
| $pH_0$ 1.6/Cl 0.05 M | 94 | 0 | 6 | 0 |
| $pH_0$ 1.6/Cl 0.02 M | 17 | 7 | 36 | 40 |
| $pH_0$ 4/Cl 0.1 M | 31 | 0 | 0 | 69 |
| $pH_0$ 4/Cl 0.05 M | 18 | 3 | 0 | 79 |
| $pH_0$ 4/Cl 0.02 M | 0 | 6 | 1 | 93 |
| $pH_0$ 6/Cl 0.1 M | 27 | 0 | 0 | 73 |
| $pH_0$ 6/Cl 0.05 M | 14 | 6 | 0 | 80 |
| $pH_0$ 6/Cl 0.02 M | 0 | 13 | 3 | 84 |
| $pH_0$ 8/Cl 0.1 M | 28 | 5 | 5 | 62 |
| $pH_0$ 8/Cl 0.05 M | 17 | 7 | 36 | 40 |
| $pH_0$ 8/Cl 0.02 M | 0 | 17 | 31 | 52 |

Figure 2.8: Rietveld refinement for precipitate at varying pH and chloride concentrations[17]

(Peretyazhko, et al. 2016)[16] looks at how the presence of sulphate affect the precipitation of akaganeite. The akaganeite were synthesised using $FeCl_3$ and varying amounts of $NaSO_4$ at different pH values. The XRD of the precipitates at the various pH values and sulphate concentrations are shown in Figure 2.9. Similarly to the XRDs without sulphate present, the akaganeite is primarily present and more crystalline at the lower pH values, the akaganeite peaks had disappeared when

the pH was 4. When the sulphate concentration was increased, the akaganeite peaks are becoming smaller and broader while the natrojarosite peaks appear and become increasingly more distinct. Figure 2.10 shows the Rietveld refinement of the phases in the XRD. Like the XRD it shows that the amount of akaganeite decreases with increasing pH and sulphate concentration. At the lowest pH the sulphate concentration could reach 0.05M before the amounts of akaganeite started to decrease. This paper shows the importance of pH and sulphate concentration on the precipitation of akaganeite and other iron hydroxides. [16]

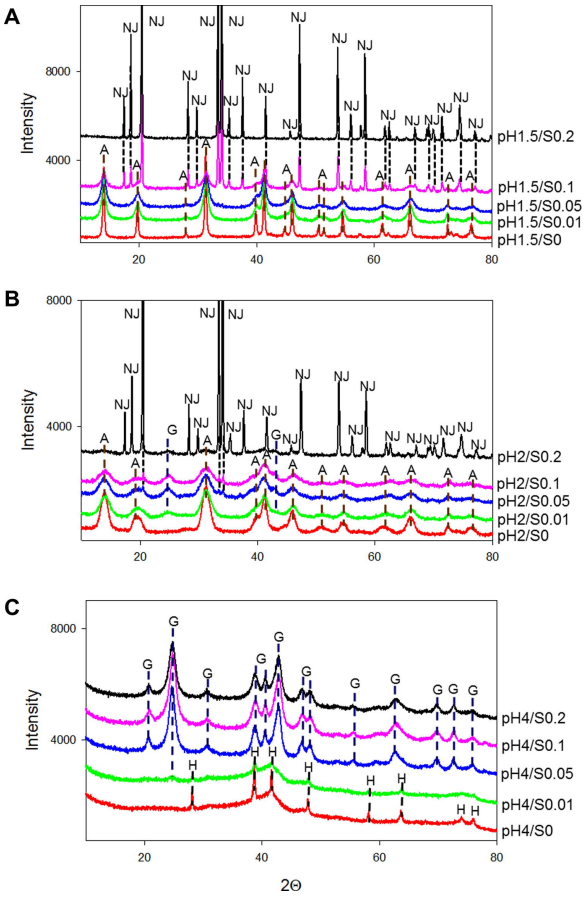


Figure 2.9: XRD of precipitate formed in the presence of variating sulphate concentrations. (a) $pH_0$ 1.5, (b) $pH_0$ 2 and (c) $pH_0$ 4. A:akaganeite; H:hematite; G:goethite; NJ:natrojarosite.[16]

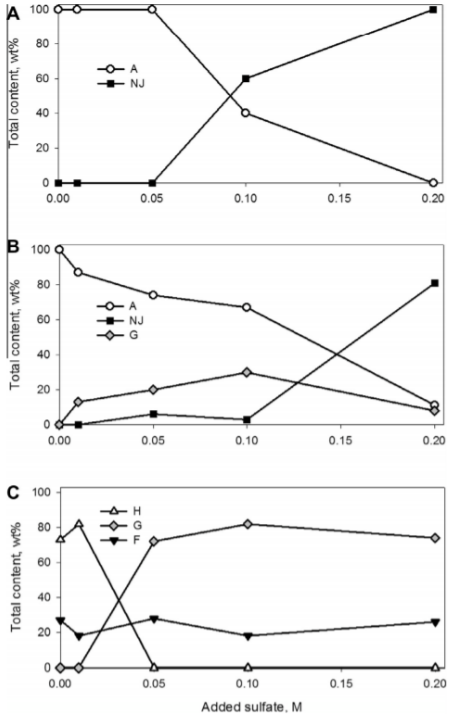


Figure 2.10: Rietveld refinement of the precipitate. (A) initial pH 1.5, (B) initial pH 2 and (C) initial pH 4. A:akaganeite; NJ:natrojarosite; G:goethite; H:hematite; F:ferrihydrite.[16]

## 2.3 Adsorption on Akaganeite

Akaganeite have tunnels that are filled with chloride to stabilise the structure. These chloride ions can be exchanged with other ions, allowing the akaganeite to remove a significant amount of ions in a solution, while releasing chloride. [14, 15]

Figure 2.11 shows the amount of chloride that got released over time when akaganeite was incubated in a solution containing anions. In addition, the peaks of the XRD of the anion exchanged akaganeite shifted, indicating a change in the structure of the akaganeite caused by the exchange. The initial release of the chloride was very rapid, after that the release flattened out after 20 hour.[14]

There are a similar result in Figure 2.12, a rapid release of chloride initially, before it starts to slow down. In this paper however the x. axis in measured in minutes. [15]

From these two papers graphs on the release of chloride, one can infer that the ability of akaganeite to remove fluoride is quite good. The difference between the F-exchange compared to the $H_2O$ exchange and blank test together with the change in XRDs of the akaganeite indicates that some of the fluoride becomes a part of the tunnel structure.

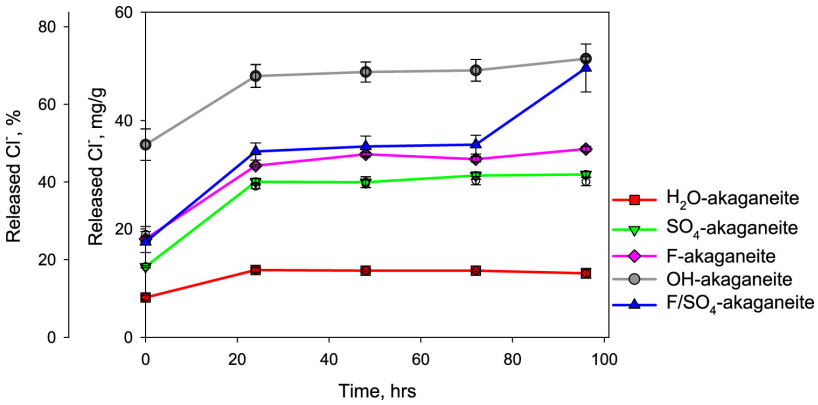


Figure 2.11: Release of chloride vs. time for Cl-akaganeite in an anion containing solutions[14]

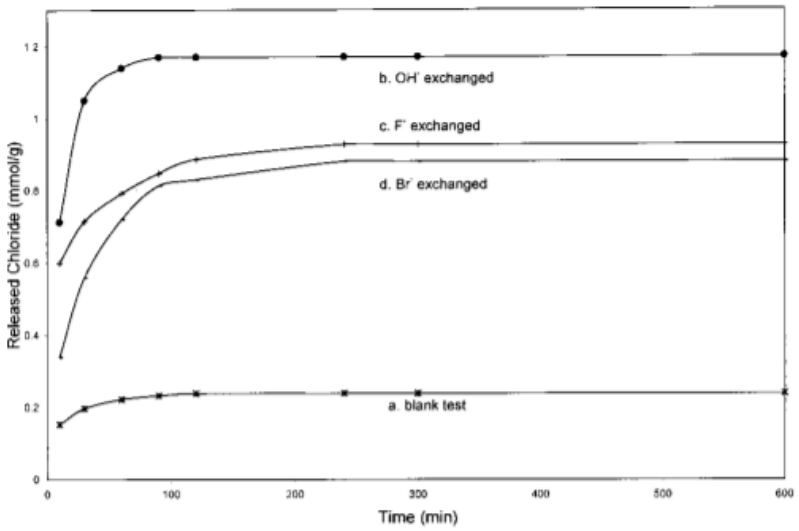


Figure 2.12: Release of chloride vs. time for Cl-akaganeite in an anion containing solutions[15]

Granular ferric hydroxide (GFH) is poorly crystalline akaganeite. It is an efficient adsorbent, including for fluoride. Kumar, et al. 2008[11], Tang, et al. 2009[12] and Pepper, et al. 2018[13] are all papers that look at the ability of the GFH to remove fluoride from solutions.Figure 2.13(Kumar, et al. 2008) shows the effect time has on the amount of fluoride adsorbed. it shows a very rapid adsorption that slows down with time, the majority of the akaganeite are adsorbed within 10 min. Figure 2.14(Tang, et al. 2009) shows the amount of fluoride adsorbed at different equilibrium pH, it shows that the adsorption starts to decrease at a pH above 6. Figure 2.15(Kumar, et al. 2008) shows the effect the temperature has on the amount adsorbed. It shows that the amount adsorbed is higher at the higher temperature. Figure 2.16(Tang, et al. 2009) shows the impact that competing anions have on the adsorption of fluoride. All the competing anions worsen the adsorption even at

the relatively low concentrations of 300mg/L. [11–13]

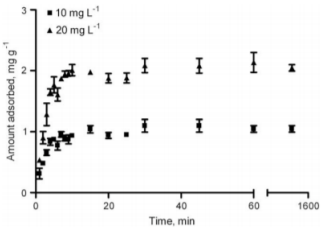


Figure 2.13: Fluoride adsorbed plotted against time for two initial fluoride concentration[11]

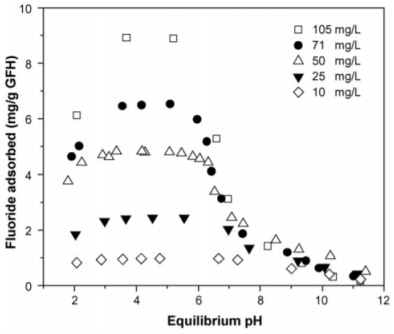


Figure 2.14: Adsorption of fluoride on GFH as functions of pH with different fluoride concentrations[12]

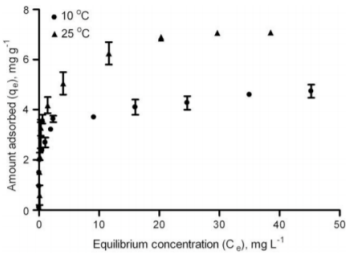


Figure 2.15: Fluoride adsorbed plotted against equilibrium concentration for two different temperatures[11]

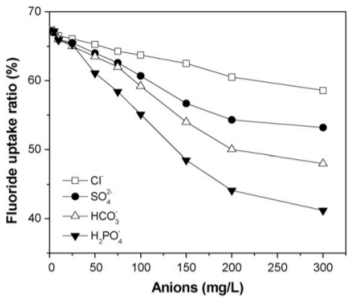


Figure 2.16: Adsorption of fluoride on GFH as a function of the concentration of competing ions[12]

# 3 Materials and Methods

## 3.1 Chemicals

The sodium fluoride(99.0-100.5%, AnalaR NORMAPUR), sodium chloride(99.5-100.5%, AnalaR NORMAPUR), Nikkel(II)sulfat heksahydrat(≥98%, GPR RECTAPUR) and Iron(II)chloride tetrahydrate (≥99.0%, Purified) were from VWR Chemicals, while sodium hydroxide(Emsure) and hydrogen peroxide(30% stabilized for synthesis) were from Merck. The Nitric acid(70%) was from Honeywell Fluka.

To make the TISAB II the following chemicals were used, sodium chloride(≥ 99.0%), acetic acid(≥99.0%), sodium hydroxide(97%) and Titriplex IV(1,2-Cyclohexanediamine-N,N,N'N'-tetraacetic acid ≥99.0%), all from Sigma Aldrich.

## 3.2 Mixed-Suspension-Mixed-Product-Removal Reactor

The main part of these experiments were done using the mixed-suspension-mixed-product-removal(MSMPR) reactor setup shown in Figure 3.1. The set up consists of one glass reactor, a refrigerated/heating circulator, three pumps with corresponding containers, Mettler Toledo SevenExcellence, a stirrer, and a computer. The reactor has a double glass wall, allowing water from the circulator to flow between the two walls, and an overflow hole that the solution will flow out when the reactor is full, causing an outflow at a constant speed and composition once steady state is reached. The advantage of using a MSMPR reactor is that it allows for easy manipulation of the steady state by altering the inlet flows, concentration, temperature and pH to closer simulate a continuous system that the industry may have.

The Mettler Toledo SevenExcellence measures the pH and oxidation potential of the solution in the reactor and sends the measured values to the computer, where they are logged using LabX. The computer controls the flow of NaOH using feedback PI control with the software LabView, where the current pH logged in LabX is compared to the pH setpoint, adjusting the NaOH flow with proportional gain(P) of 30 and integral time(I) of 1.3.

The individual pump, to the left, is pumping $H_2O_2$ at a constant flow into the reactor to oxidate the ferrous iron and one of the pumps to the right is pumping NaF, NaCl, $FeCl_2$*$4H_2O$ and $NiSO_4$*$6H_2O$ with a constant flow. The last pump transports NaOH to control the pH in the reactor with a pump speed that varies and is controlled by the computer. The stirrer is set at a speed of 500 rpm and ensures that the solution in the reactor is mixed.

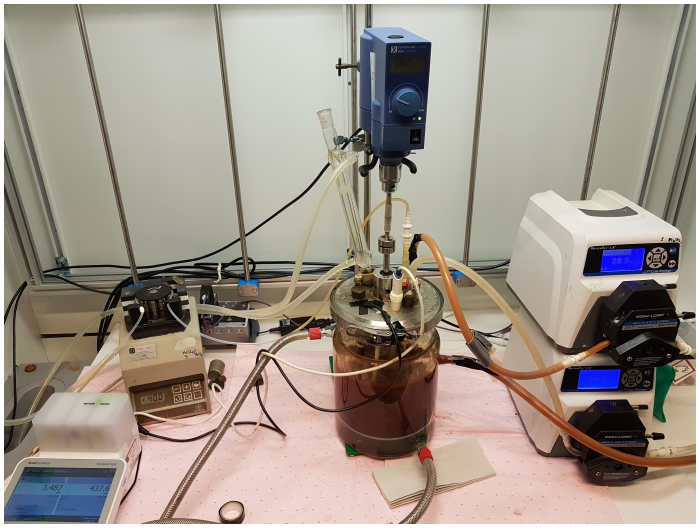

Figure 3.1: The MSMPR Setup

### 3.2.1 Experimental

To evaluate the effect and interactions of temperature, residence time and concentration of sulphate had on the fluoride removal, a design of experiment(DOE) was made with these as variables. The temperature had two levels, 25°C and 60°C. The residence time, like temperature, had two levels, 30 minutes and 45 minutes. In the DOE, there were three levels used for the concentration of sulphate, 0, 10 and 20 g/L. The resulting DOE is shown in Table 3.1.

Table 3.1: Design of Experiments

| Name | T[°C] | $\tau$ [min] | $SO_4$ [g/L] |
|---|---|---|---|
| $E_{60;30;0}$ | 60 | 30 | 0 |
| $E_{60;30;10}$ | 60 | 30 | 10 |
| $E_{60;30;20}$ | 60 | 30 | 20 |
| $E_{60;45;0}$ | 60 | 45 | 0 |
| $E_{60;45;10}$ | 60 | 45 | 10 |
| $E_{60;45;20}$ | 60 | 45 | 20 |
| $E_{25;30;0}$ | 25 | 30 | 0 |
| $E_{25;30;10}$ | 25 | 30 | 10 |
| $E_{25;30;20}$ | 25 | 30 | 20 |
| $E_{25;45;0}$ | 25 | 45 | 0 |
| $E_{25;45;10}$ | 25 | 45 | 10 |
| $E_{25;45;20}$ | 25 | 45 | 20 |

The experiments are partially modelled after the concentrations that Nikkelverk have. The common concentration in their process stream is 7-15 g/L of iron and 40 g/L of sulphate. To reduce the chemicals needed the concentrations were halved, therefore the experiments were run aiming at a concentration of 5 g/L of iron and a max concentration of sulphate of 20 g/L in the reactor.

Based on the project work "Study of Parameters on Fluoride Removal in Industrial Applications" with this reactor and a similar reaction, the $H_2O_2$ pump was set to 7 mL/min and 10.5 ml/min for a residence time of 45 min and 30 min respectively, while the NaF-NaCl- $FeCl_2$-$NiSO_4$ pump was set 19 mL/min and 28.5 mL/min for a residence time of 45 min and 30 min respectively. The target molar ratio of $H_2O_2$:Fe is 1:1, giving the target of 0.09 mol/L, while the target for NaOH was 0.175 mol/L. To obtain these concentrations, 163 g of 30% $H_2O_2$ was weighed out in the $H_2O_2$ container and diluted to 2.5 L with de-ionized water, while 100 g of NaOH was weighed out in the NaOH container and diluted to 6 L with de-ionized water.

Because of sulphate hindering the precipitation of akaganeite, while chloride facilitates it, NaCl was added to the reactor to improve the precipitation of akaganeite. The amount of added chloride was set such that the highest sulphate/chloride ratio was equal to the ratio at 0.10 M sulphate in Figure 2.10. Therefore 1035 g of NaCl was weighed out in the NaF-NaCl- $FeCl_2$-$NiSO_4$ container. In the earlier experiments, the concentration of fluoride had been 10 mg/L and almost everything had been removed by the precipitate, therefore the concentration of fluoride in these experiments were increased to 100 mg/L. To get the desired concentration of fluoride, iron and sulphate, 3.1413 g NaF, 253 g $FeCl_2$*$4H_2O$ and 0, 389 or 777 g $NiSO_4$*$6H_2O$ were also weighed out in the NaF-NaCl-$FeCl_2$-$NiSO_4$ container before it was diluted to 6 L with de-ionized water.

When the MSMPR reactor had reached steady state, identified by the pH and oxidation potential being constant, 200 mL of the outflow was gathered and filtrated using vacuum filtration with blue ribbon filtration paper from Scleicher & Scuell. The filtrate was then filtered through a 0.22 µm Millipore membrane filter. The filter paper and membrane filter were placed on watch glasses and dried in an oven for 2 days at 40°C. After the drying, the precipitate was crushed using a pestle and mortar. The ions in the filtrate after the membrane filtration was quantified using the methods in subsection 3.4 and 3.6.

## 3.3 X-ray Diffraction

The precipitate from subsubsection 3.2.1 was characterized using X-ray diffraction(XRD). Due to equipment downtime, the precipitate was characterized using two different XRD machines.

$E_{60;30;0}$, $E_{60;45;0}$, $E_{25;30;0}$, $E_{25;45;0}$, $E_{60;30;10}$, $E_{60;30;20}$ and $E_{25;30;10}$ were characterized using a Bruker D8-focus with CuK$\alpha$ radiation, in the range of 10-80°, with a step size of 0.02°, step time of 2.5 s and a divergence slit of 0.200 mm, using standard sample holders at ambient conditions and correcting the diffractogram for iron fluorescence. $E_{60;45;10}$, $E_{60;45;20}$, $E_{25;30;20}$, $E_{25;45;10}$ and $E_{25;45;20}$ were characterized using a Bruker D8 A25 Davinci with CuK$\alpha$ radiation, in the range of 10-80°, with a step size of 0.013°, step time of 0.68 s and a variable divergence slit "V6", meaning that the illuminated length on the sample stays at 6 mm, using back loader sample holders at ambient conditions. Diffrac.EVA V5.2 and "Crystallography Open Database (REV212673 2018.12.20)" were used to determine the phases present in the precipitate.

To estimate the percentages of different iron and NaCl precipitates in the product, Rietveld refinement in the software Topas were used. Rietveld refinement uses the position, width and intensity of the peaks, together with the structure of the crystals present, to estimate how much of the precipitate that is made up of each crystal. The structures of the crystals used in the refinement were "00-042-1315" for akaganeite, "00-005-0628" for NaCl, "01-085-6816" for natrojarosite and "00-033-0664" for hematite using the database PDF-4+. This database did not have the structure for schwertmannite, therefore the structure of schwertmannite was obtained from Matteo Sestu(2015)[21].

## 3.4 Fluoride Ion Quantification

To quantify the amount of fluoride in the filtrate from subsection 3.3 and subsection 3.5, a fluoride selective electrode shown in Figure 3.2 was used. Using a fluoride selective electrode is a quick and straightforward way to measure the fluoride concentration in a solution with a measuring range from 0.02 mg/L to saturated solution. It works by measuring the electrode potential of a sample and comparing it to a calibration curve made with known concentrations and is related to the fluoride activity by Nernst equation:

$$E = E_0 + 2.3\frac{RT}{nF}log(a) \tag{3.1}$$

where $E_0$ is a constant for a given cell, $R$ the gas constant, $n$ the ionic charge, $F$ the Faraday constant and $a$ is the activity. This means that the calibration curve for fluoride, with n=1, at ambient temperature of 298K has a theoretical slope of 59.16 mV.

To make the calibration curve, a standard solution of fluoride with a concentration of 1000 mg/L was series diluted to 200 mg/L, 20 mg/L, 2 mg/L and 0.2 mg/L. 20 mL of each of these concentrations were mixed with 20 mL total ionic strength adjustment buffer(TISAB II), giving four samples with known concentrations of 100 mg/L, 10 mg/L, 1 mg/L and 0.1 mg/L. Using the fluoride selective electrode, the electrode potential was measured for each of these four known concentrations and from this the calibration curve shown in Figure 3.3 were made, the values measured can be found

Figure 3.2: Fluoride Ion Quantification Setup

in the excel file linked in Appendix A. In Figure 3.3 the x-axis is log(c) of the TISAB-sample mix, while the y-axis is the measured potential.

The TISAB II used in the fluoride quantification was made in the lab. It was prepared in a 2L solution by the following recipe: 8 g of titriplex IV, 116 g of NaCl and 114 mL of acetic acid were mixed and diluted with de-ionized water to approximately 1L. The pH of this mix was adjusted to 5.4 using 5 M NaOH and then diluted with de-ionized water to a total of 2 L.

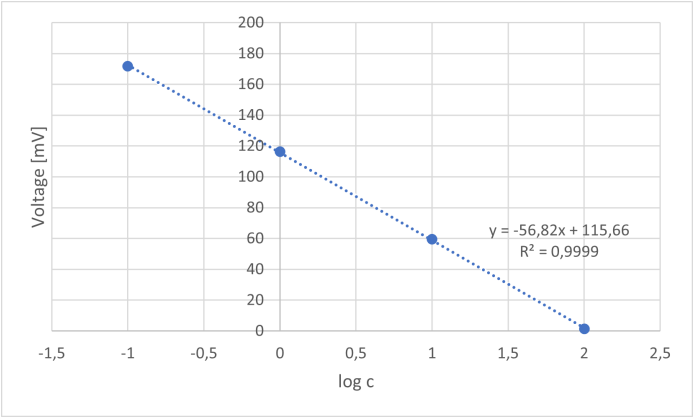


Figure 3.3: Fluoride Selective Electrode Calibration Curve

To calculate the concentration of fluoride in the solution 20 mL of sample were mixed with an

equal amount of TISAB II, and the electrode potential was measured. By using the calibration curve and the measured electrode potential, the concentration of the sample were calculated.

## 3.5 Washing and Dissolving of Precipitate

Around 1 gram of the precipitate from subsubsection 3.2.1 was weighed out and washed in 20 mL of de-ionized water in a beaker with a stirring magnet. After an hour, the solution was filtrated and diluted to 30 mL. The fluoride content in the filtrate was quantified using the fluoride ion quantification in subsection 3.4. , while the solid was dried for 24 hours in a fume hood and then weighed.

14.3 mL of the 70% nitric acid was diluted with de-ionized water in a 1 L volumetric flask to get a 1% nitric acid solution.

The solid after washing was added to an Erlenmeyer flask together with a magnet and 20 mL of the 1% w/V nitric acid to dissolve part of the solid. The flask was placed in a waterbath at 70°C for 45min. The sample was then cooled down and filtrated and the filtrate was diluted to 30 mL. The solids after filtration were taken through this process twice more while the filtrate was measured for fluoride as described in subsection 3.4.

## 3.6 Microwave Plasma Atomic Emission Spectroscopy

The concentration of sodium, iron, nickel and sulphur were measured using Microwave Plasma Atomic Emission Spectroscopy(MP-AES). The MP-AES used for these measurements was the Agilent 4210 MP-AES, shown in Figure 3.4, it works by comparing the intensity of the plasma at certain wavelengths compared to a calibration curve. The calibration curve for the metal analysis was made using known concentrations of 50, 10, 5, 2.5, 1 and 0 mg/L, while the calibration curve for sulphur analysis used the concentrations of 1000, 100, 10, 1 and 0 mg/L.

The samples from subsubsection 3.2.1 were diluted 100 times to get the concentration inside of the calibration curve.

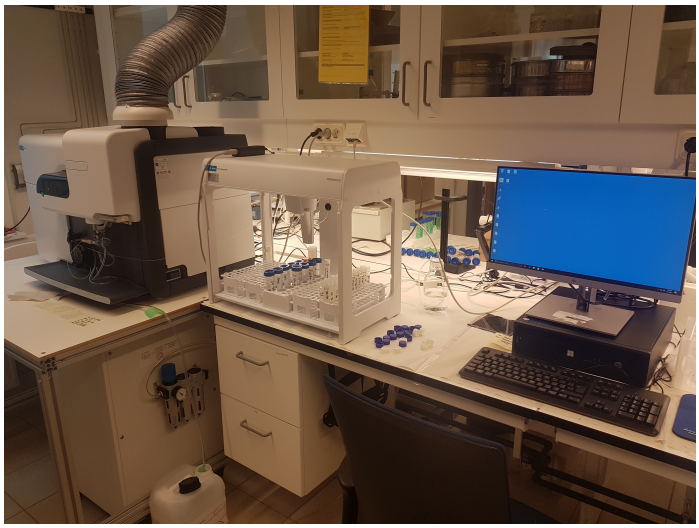

Figure 3.4: MP-AES agilent 4210

# 4 Results and Discussion

This chapter shows the results from the XRD characterization of the precipitate, the results from the fluoride selective electrode and MP-AES on the filtrate, and the results from the washing and dissolving of the precipitate. The results in excel file are given in Appendix A. The experiments were done as described in subsubsection 3.2.1. However, of note was that the filtrations of the experiments that included sulphate were drastically faster than the filtrations of the 4 without sulphate.

## 4.1 Characterization of the Precipitate

The XRDs from subsection 3.3 are shown in Figure 4.1, 4.2, 4.3 and 4.4. Each of the figures shows the XRDs of the three experiments done at each temperature and residence pair with varying $SO_4$ levels. Figure 4.1 and 4.2 shows the XRDs for the precipitation at a temperature of 25°C, it shows that the akaganeite peaks primarily are visible for the precipitates without any sulphate present, this can be explained by the presence of sulphate preventing the precipitation of akaganeite in accordance with the theory in subsubsection 2.2.1 and with the increasing sulphate concentration the peaks corresponding to schwertmannite, a iron-oxyhydroxysulfate similar to akaganeite in structure but with sulphate in the tunnels instead of chloride, increase. The XRD also shows that the peaks are quite broad and low, with the exception of the sodium chloride peaks, indicating that the precipitate has a quite amorphous crystal structure, again this corresponds to the theory in subsection 2.2 as the low temperatures cause a higher supersaturation which in turn results in a fast, less uniform precipitation.

Comparing the XRDs of the precipitates at 60°C shown in Figure 4.4 and 4.3 it is apparent that the precipitate is both more crystalline and have the akaganeite peaks, albeit small ones, at all the $SO_4$ concentrations. The increased crystallinity can be explained by the increased temperature, causing a lower supersaturation and thus less nucleation, causing the number of crystals to decrease such that the slow crystalline growth in dominates. In these diffractions, it is also visible that the schwertmannite peaks become taller with the increasing concentration of sulphate.

The last point of interest with these XRDs are the fact that out of the twelve of them, only three are lacking the sodium chloride peaks. This can not have been caused by the rinsing technique changing over time, as one of them was done early in the experiments and the last two were done late. It also can not be explained by the nature of the precipitate as they differ, it is therefore probably due to the randomness of some samples clinging to the walls of the Büchner funnel and thus getting rinsed a bit more.

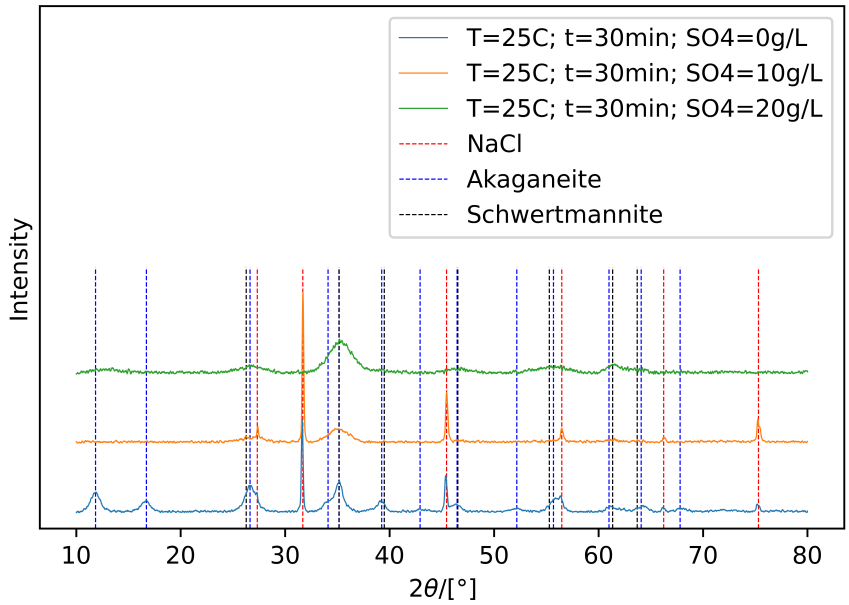


Figure 4.1: XRD of $E_{25;30;0}$, $E_{25;30;10}$ and $E_{25;30;20}$

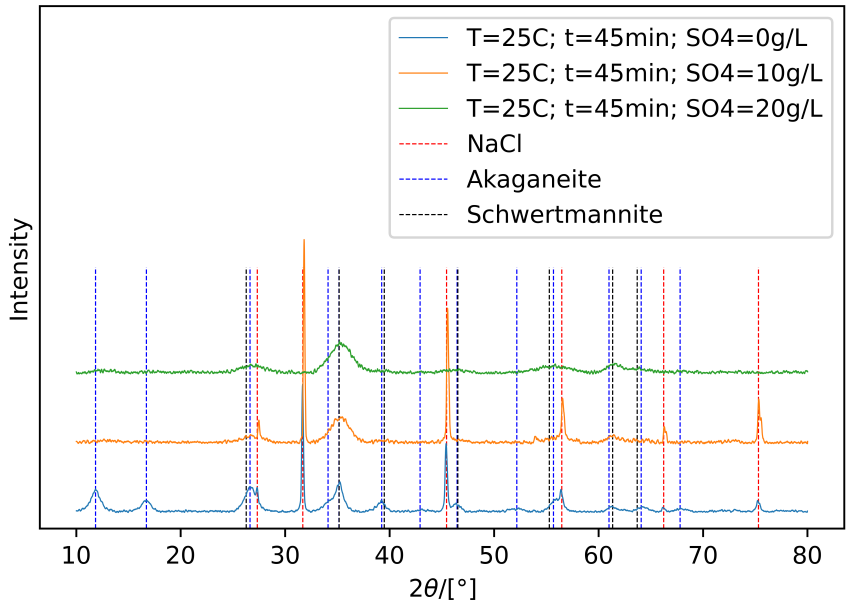


Figure 4.2: XRD of $E_{25;45;0}$, $E_{25;45;10}$ and $E_{25;45;20}$

Table 4.1 shows the resulting Rietveld refinement of the precipitate following the method described in subsection 3.3. Initially, the refinement was done including hematite and natrojarosite, but as

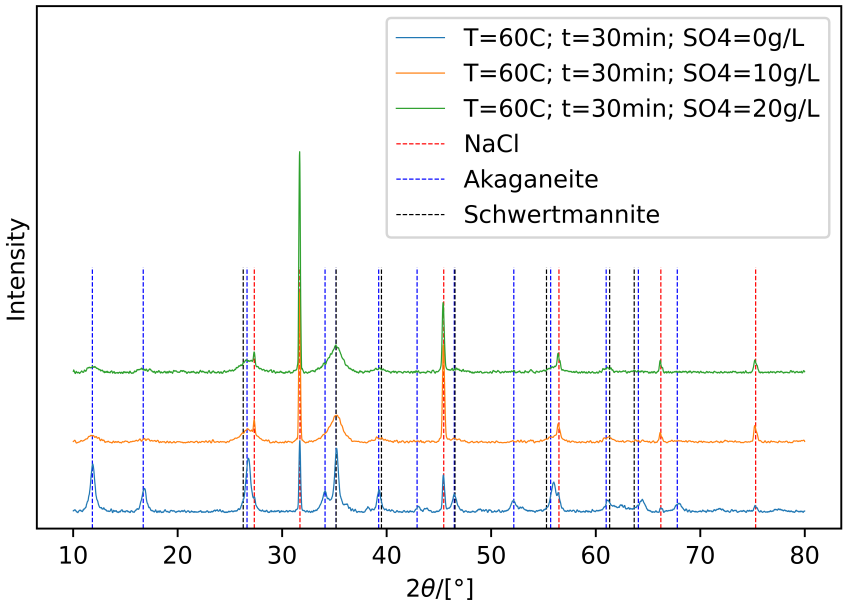


Figure 4.3: XRD of $E_{60;30;0}$, $E_{60;30;10}$ and $E_{60;30;20}$

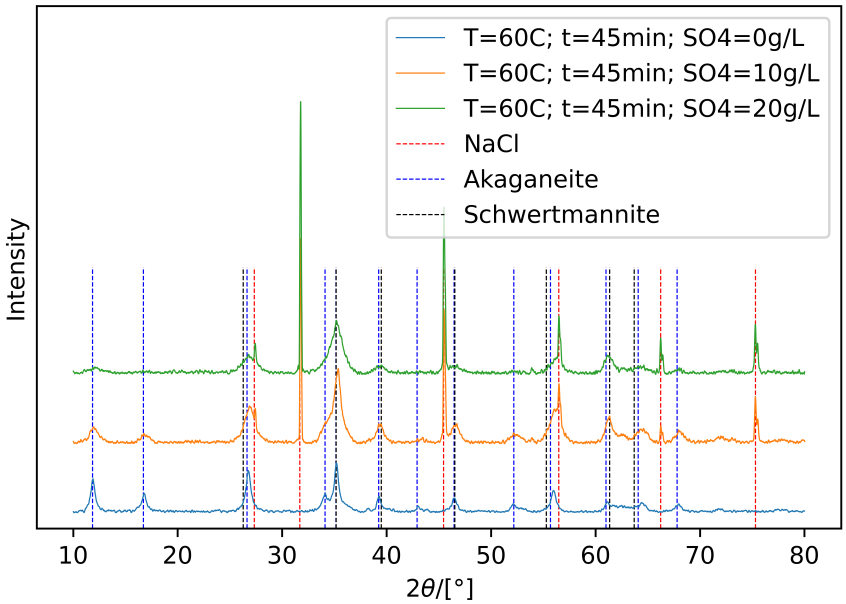


Figure 4.4: XRD of $E_{60;45;0}$, $E_{60;45;10}$ and $E_{60;45;20}$

they remained at less than 1% throughout the refinements, their structures were removed to prevent them from causing interference. In addition when no $NiSO_4$ was added, the schwertmannite

structure was also removed. In the table akag. is akaganeite, schw. is schwertmannite and Ferri. is ferrihydrite. Important to remember that it is the composition of the crystalline part that is estimated.

The Rwp is an estimate of how good of a fit the Rietveld refinement is, with lower values indicating a better fit, a value below five generally indicates that the diffractogram is of sufficient quality and that the refinement has yielded an accurate estimate. In the table, we can see that seven of the twelve have Rwp values below five, the seven done using the D8-focus, while the five that have Rwp above five were done using the Davinci. This means that there are only one set of temperature-residence time pairs that have an accurate estimate for all sulphate concentration, the one at 60°C and 30 min.

The crystallinity column is an estimate of the percentage of the precipitate that is crystalline, the remanding being amorphous. These values are obtained from Diffrac.EVA V5.2 and therefore not affected by the Rietveld refinement, although the Rwp values, as mentioned, are also partially an indication of the quality of the diffractogram, thus indicating a less accurate estimated crystallinity. Because the NaCl in the precipitate is significantly more crystalline compared to the other phases, in addition to it not being of much interest, it has been deducted in the column crystallinity without NaCl. It confirms the visual changes in crystallinity in the XRDs, all of the precipitates are relatively crystalline when no sulphate are added and Figure 4.1, 4.2 and 4.3 have similar crystallinity at both 10 and 20 g/L sulphate, while Figure 4.4 shows a significant decrease in the crystallinity between 10 and 20 g/L of sulphate which corresponds to the drop from 51% to 43% in Table 4.1. It would appear that the crystallinity is mostly dependent on whether or not there is sulphate present coupled with the temperature. Leaving out $E_{60;45;20}$, the values for crystallinity are around 60% when there are no sulphate present, regardless of temperature, while when there are sulphate present, the crystallinity varies with temperature, being around 49% at 60°C while it is around 39% at 25°C. This indicates that sulphate and the interaction between sulphate and temperature have a significant impact on the crystallinity, while temperature alone has a lesser importance. The estimated amounts of NaCl in Table 4.1 corresponds quite well to the XRDs. The trend of the crystallinity decreasing when the experiments are done at 25°C compared to the ones done at 60°C corresponds to the difference in supersaturation, leading to different crystallization speed and thus a higher crystallinity at the lower supersaturation.

The experiments done at 0 g/L of sulphate indicate that the crystalline precipitation of akaganeite is favoured over the crystalline precipitation of ferrihydrite, while $E_{60;30;10}$ and $E_{60;30;20}$ indicate that the schwertmannite precipitation gets favoured over the precipitation of akaganeite. This gives the following favoured precipitation, akaganeite$\gg$ferrihydrite at 0 g/L of sulphate, schwertmannite$>$

akaganeite≫ ferrihydrite at 10 g/L of sulphate and schwertmannite≫akaganeite≈ferrihydrite at 20 g/L of sulphate. The estimated amounts of NaCl in Table 4.1 corresponds quite good to the visual look of the XRDs, in particular that $E_{60;45;0}$, $E_{25;45;10}$ and $E_{25;45;20}$ don't have any NaCl peaks and also have no NaCl estimated by the Rietveld refinement.

Table 4.1: Rietveld Refinement of Precipitate

| | Akag.[%] | NaCl[%] | Schw.[%] | Ferri.[%] | Rwp | crystallinity[%] | crystallinity[%] without NaCl |
|---|---|---|---|---|---|---|---|
| $E_{60;30;0}$ | 71.99 | 10.63 | 0 | 17.38 | 4.197 | 71 | 63 |
| $E_{60;30;10}$ | 33.66 | 17.97 | 44.78 | 3.59 | 4.565 | 58 | 48 |
| $E_{60;30;20}$ | 3.82 | 17.61 | 75.58 | 3.00 | 4.049 | 60 | 49 |
| $E_{60;45;0}$ | 77.43 | 0.1 | 0 | 22.47 | 4.591 | 62 | 62 |
| $E_{60;45;10}$ | 10.85 | 9.52 | 43.2 | 36.42 | 10.961 | 56 | 51 |
| $E_{60;45;20}$ | 6.19 | 12.05 | 40.93 | 40.83 | 8.914 | 49 | 43 |
| $E_{25;30;0}$ | 78.02 | 13.67 | 0 | 8.31 | 3.537 | 70 | 60 |
| $E_{25;30;10}$ | 41.52 | 22.22 | 36.26 | 0 | 4.956 | 54 | 42 |
| $E_{25;30;20}$ | 4.25 | 0 | 49.92 | 45.83 | 9.156 | 39 | 39 |
| $E_{25;45;0}$ | 75.21 | 18.8 | 0 | 5.99 | 3.498 | 72 | 58 |
| $E_{25;45;10}$ | 15.68 | 10.22 | 36.81 | 37.19 | 8.370 | 42 | 38 |
| $E_{25;45;20}$ | 0 | 0 | 48.79 | 51.21 | 9.065 | 36 | 36 |

The change in akaganeite and schwertmannite concentration are shown in Figure 4.5. As previously discussed, the one at 60°C and residence time of 30 min are the only one that is accurate for all three sulphate concentrations. It shows a trend with decreasing amounts of akaganeite and increasing amounts of schwertmannite when the sulphate concentration increases, this is in agreement with the theory that sulphate hinders precipitation of akaganeite and is required for the precipitation of schwertmannite. It forms a very similar graph to Figure 2.10, except that they precipitated natrojarosite instead of schwertmannite. The difference in the precipitate is most likely due to the experiments in Figure 2.10 lasting 5 h, while our experiments only had a residence time of 30 or 45 min. The reason for the time affecting the precipitate is that schwertmannite is a metastable phase that can transform to goethite or jarosite over time. Although the remaining three graphs include less accurate estimates, they still show the general trend with increasing amounts of schwertmannite and decreasing amounts of akaganeite.

In addition to estimating the percentages of each structure in the precipitate, the lattice param-

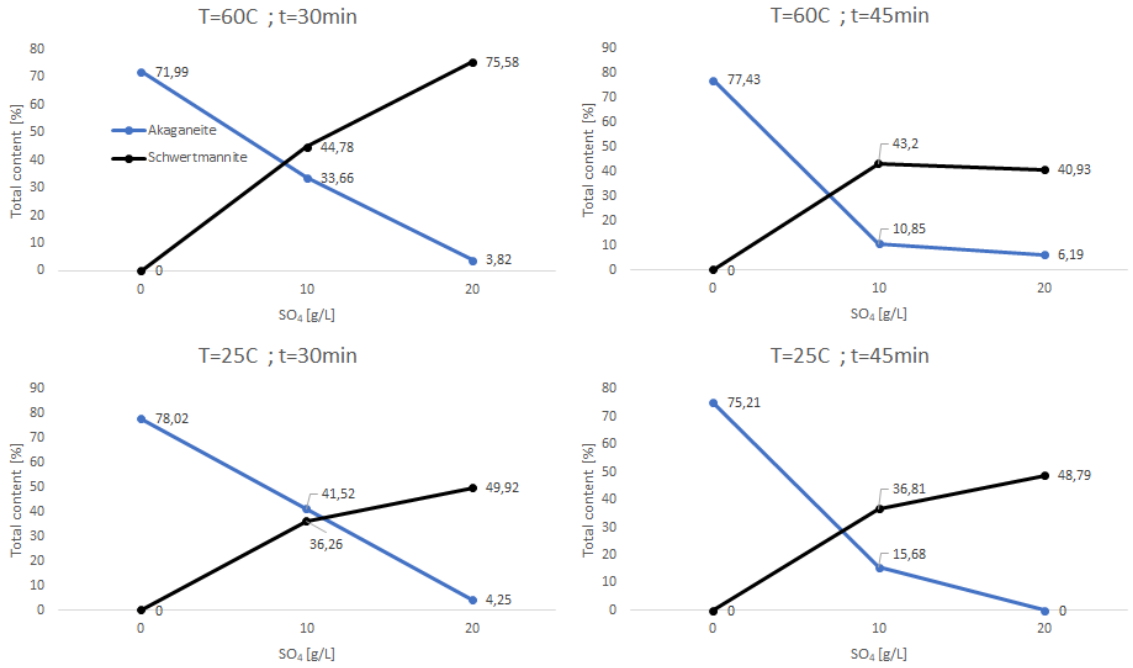


Figure 4.5: Quantities of akaganeite and schwertmannite in precipitate identified with Rietveld refinement

eters were also refined. The resulting cell parameters are shown in Table 4.2. Unlike the solids used to refine the parameters in Figure 2.2, the precipitate in our experiments consists of multiple phases that shares similar peaks, thus the refinement will probably be less accurate. Looking at $E_{60;30;0}$ and $E_{60;45;0}$, they both have b values that are close to the akaganeite one, a and c values between that of Cl-akaganeite and F-akaganeite and no sulphate present, this is a slight indication that some of the fluoride is indeed in the tunnels and not just on the surface, although not a conclusive proof. Of the remaining one, $E_{60;45;10}$ also have b values that are close to the akaganeite one, a and c values between that of Cl-akaganeite and F-akaganeite and no sulphate present, but it is one of the inaccurately measured. The rest have one or more values outside of the wanted area to compare with Figure 2.2 and will therefore be of little help to determine if any of the fluoride is located inside of the tunnel structure of akaganeite or not.

Table 4.2: Rietveld Refinement of Precipitate Lattice Parameters

| | a [Å] | b [Å] | c [Å] |
|---|---|---|---|
| $E_{60;30;0}$ | 10,5325406 | 3,03168860 | 10,5267657 |
| $E_{60;30;10}$ | 10.9069015 | 3.0047075 | 10.5627955 |
| $E_{60;30;20}$ | 10.6311177 | 3.0310937 | 10.5079554 |
| $E_{60;45;0}$ | 10.5296792 | 3.0321018 | 10.5223953 |
| $E_{60;45;10}$ | 10.5197205 | 3.0274436 | 10.5159891 |
| $E_{60;45;20}$ | 10.4468361 | 3.0336556 | 10.4103081 |
| $E_{25;30;0}$ | 10.5829900 | 3.0338543 | 10.5538635 |
| $E_{25;30;10}$ | 10.5709661 | 3.0464523 | 11.3316774 |
| $E_{25;30;20}$ | 11.6775362 | 2.8429594 | 11.2781107 |
| $E_{25;45;0}$ | 10.5851996 | 3.0348667 | 10.5364304 |
| $E_{25;45;10}$ | 10.6406620 | 3.0434575 | 10.5274041 |
| $E_{25;45;20}$ | 10.0907553 | 3.1644817 | 10.0059060 |

## 4.2 Quantification of Filtrate from Reactor

The filtrates are shown in Figure 4.6 and 4.7. In Figure 4.6 the following filtrates are shown, $E_{60;30;0}$, $E_{60;30;10}$, $E_{60;30;20}$, $E_{60;45;0}$, $E_{60;45;10}$ and $E_{60;45;20}$ from the left to right. Figure 4.7 shows the following filtrates from left to right, $E_{25;30;0}$, $E_{25;30;10}$, $E_{25;30;20}$, $E_{25;45;0}$, $E_{25;45;10}$ and $E_{25;45;20}$.

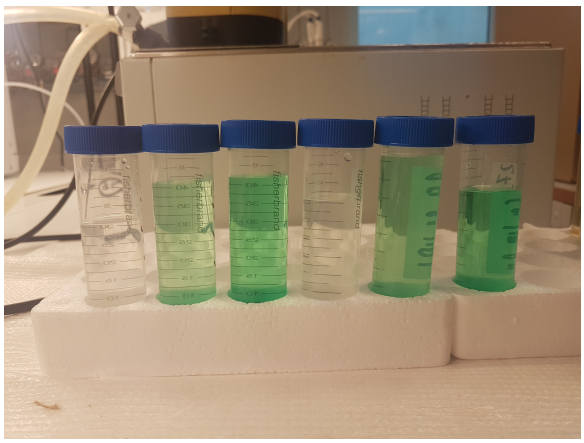

Figure 4.6: Filtrates at 60°C. From left to right: $E_{60;30;0}$, $E_{60;30;10}$, $E_{60;30;20}$, $E_{60;45;0}$, $E_{60;45;10}$ and $E_{60;45;20}$.

The colouring of the filtrates with sulphate comes from the nickel sulphate that was added, that the ones at 20 g/L are stronger coloured compared to the ones with 10 g/L means that they still contain

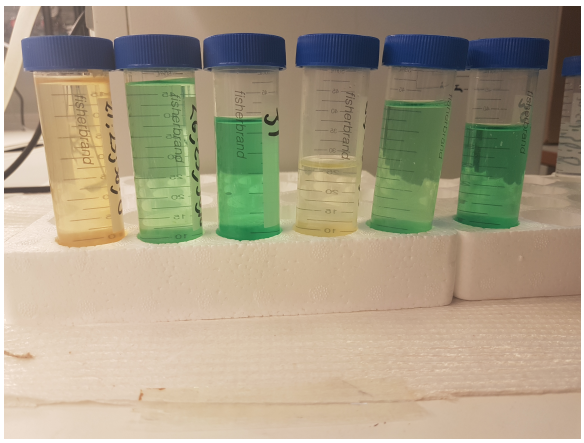


Figure 4.7: Filtrates at 25°C. From left to right: $E_{25;30;0}$, $E_{25;30;10}$, $E_{25;30;20}$, $E_{25;45;0}$, $E_{25;45;10}$ and $E_{25;45;20}$

more nickel sulphate. The yellow discolouring of the two without any sulphate added is probably caused by iron ions, as they make solutions have a yellow discolouring.

The amount of fluoride in the filtrate from the reactor was quantified using the fluoride selective electrode method described in subsection 3.4 while the nickel, iron and sulphur concentrations were determined using the MP-AES method described in subsection 3.6. Because the sulphur has such a low intensity, it can not make the calibration curve as all the intensities become close to zero without any trend. The nickel and iron, on the other hand, have an adequate intensity for an accurate calibration curve to be made.

The initial concentration of iron in the reactor was 5 g/L. The column for iron amounts left in the filtrate shows that most of the iron had precipitated when the product was removed at steady state. The iron left in the filtrate is plotted against crystallinity in Figure 4.8, it shows that there is a correlation between the crystallinity and the amount of iron that does not precipitates, although the crystallinity is related to whether or not there are sulphate present and the temperature when there is sulphate present. That the two without sulphate and at 25°C contained more iron than the two at 60°C indicated that the earlier assumption about the reason for the discolouring was correct.

The calculated amount of nickel in the reactor is 0, 6104.72, 12209.45 mg/L for 0, 10, 20 g/L of sulphate, respectively. The measured values of nickel at 0 g/L of sulphate, when no nickel has been added, is practically 0. The small deviation could be caused by impurities in the iron or an inaccurate calibration curve at low concentrations. With the presence of $NiSO_4$ in the reactor, however there is an interesting development, the amount of nickel in the filtrate varies based on the

temperature. At 25°C the amount of nickel in the filtrate is a fair bit lower than the amount of nickel added to the reactor, while at 60°C the amount are close to the calculated value, although at 10 g/L it is a bit higher, the higher concentration might simply be caused by the NaOH pump not being constant, and would be 0-2 ml/min below the wanted speed at steady state, meaning that the real concentrations in the reactor can be a bit higher than the target concentrations. It might also be caused by iron having a wavelength close to the wavelength for nickel, and therefore, the measured amount of nickel gets increased when there is more iron left in the filtrate. The NaOH pump, however, was never above the desired pump speed at steady state, meaning that the real concentrations should never be lower than the calculated ideal concentration. Because of this, the lower concentration of nickel at 60°C indicate, either that some of the nickel has precipitated, or that the concentrations in the NaF, NaCl, $FeCl_2$*$4H_2O$ and $NiSO_4$*$6H_2O$ tank is not entirely uniform. The results would lean more towards the latter, due to no nickel being identified in the XRDs and that the tank is quite large, so that despite it having a magnet stirrer, some of the dissolved elements sink more towards the bottom. Both of the varying nickel values indicates that the real concentration in the reactor is around ±10% of the calculated ideal one.

Figure 4.8 also shows the remaining fluoride plotted against the crystallinity of the precipitate and like iron, it would appear that there is a correlation between the two. As the crystallinity decreases, the amount of fluoride left in the filtrate increases, very similarly to the iron. This might just be due to the different percentages of iron precipitates, but it might also be a slight indication that the precipitate actually adsorbed some of the fluoride into the tunnel structure, as this would require a more crystalline precipitate.

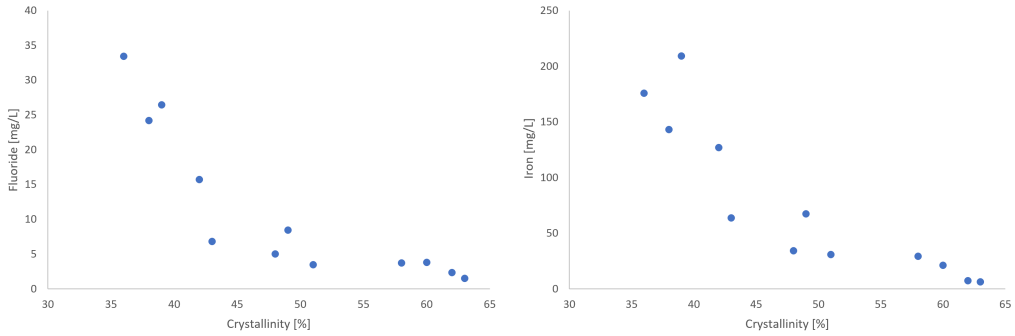


Figure 4.8: To the left crystallinity vs. fluoride, on the right crystallinity vs. iron

The remaining fluoride in the filtrate are given in Table 4.3 while Figure 4.9 and 4.10 shows the main effect plots and interaction plots. The main effect plots in Figure 4.9 shows that the residence time had a small effect compared to the other two factors, while both the temperature and sul-

Table 4.3: Quantification of Filtrate from Reactor

| T[°C] | $\tau$ [min] | $SO_4$ [g/L] | F [mg/L] | Ni [mg/L] | Fe [mg/L] |
|---|---|---|---|---|---|
| 60 | 30 | 0 | 1.59 | 0.52 | 6.35 |
| 60 | 30 | 10 | 5.02 | 5904.09 | 34.22 |
| 60 | 30 | 20 | 8.48 | 11307.42 | 67.42 |
| 60 | 45 | 0 | 2.38 | 0.52 | 7.37 |
| 60 | 45 | 10 | 3.49 | 5948.65 | 30.94 |
| 60 | 45 | 20 | 6.83 | 11316.65 | 63.85 |
| 25 | 30 | 0 | 3.82 | 0.77 | 21.22 |
| 25 | 30 | 10 | 15.71 | 6452.29 | 127.04 |
| 25 | 30 | 20 | 26.46 | 12196.86 | 209.38 |
| 25 | 45 | 0 | 3.73 | 4.13 | 29.50 |
| 25 | 45 | 10 | 24.22 | 6229.29 | 143.34 |
| 25 | 45 | 20 | 33.43 | 12279.86 | 175.74 |

phate concentrations had a significant effect on the amount of fluoride that was left in the filtrate. The interaction plots in Figure 4.10 also shows that there is little interaction between the residence time and the two other factors as the plots are close to being parallel, while there is a significant interaction between the temperature and the sulphate concentrations. The results show that with decreasing temperatures and increasing sulphate concentrations, the fluoride left increases, particularly if both the temperature is decreased and sulphate concentration increases.

The desired result is to remove as much fluoride as possible with the precipitation. Therefore, it is clear that inside the experiments' parameter values, the desired point to be at is a temperature of 60°C and 0 g/L of sulphate and a residence time of 45 min, although the last one is of less importance. Of these variables, however, the ones that can easily be manipulated is the temperature and residence time, the sulphate concentration is something that is decided by the input and less something that is controlled. Outside of the cube formed by the DOE, the effect is more uncertain, in particular, decreasing the residence time will probably start having a significant detrimental effect on both the amount of iron precipitated and the fluoride removal, while increasing the temperature should work fine until it starts to cause problems due to boiling and evaporation.

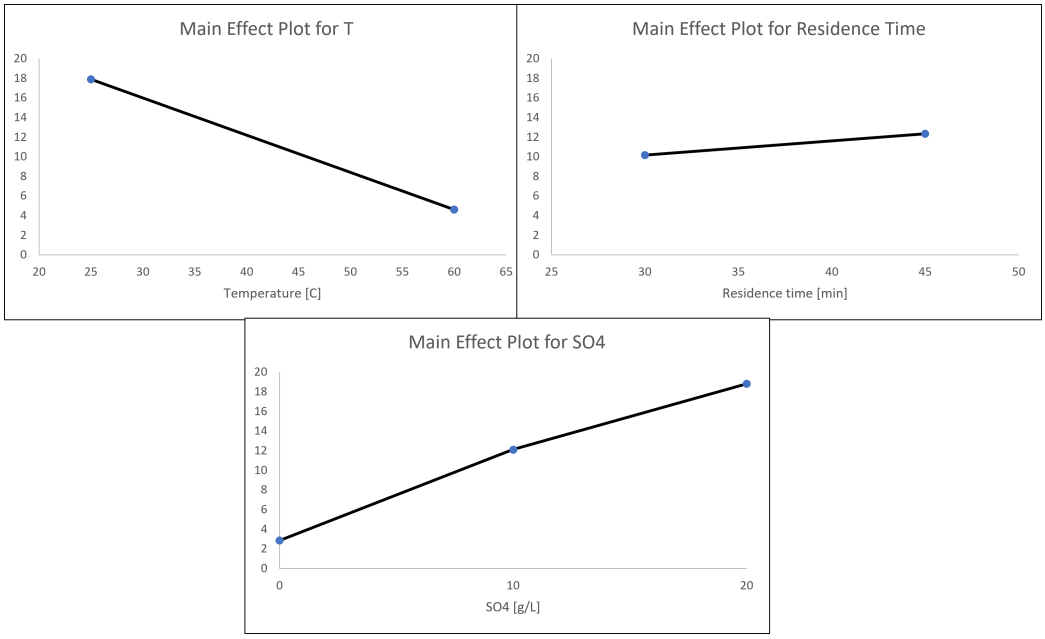


Figure 4.9: Top left: main effect plot for temperature, top right: main effect plot for residence time, bottom: main effect plot for sulphate concentration. For all of them the Y-axis is the amount of fluoride in the filtrate

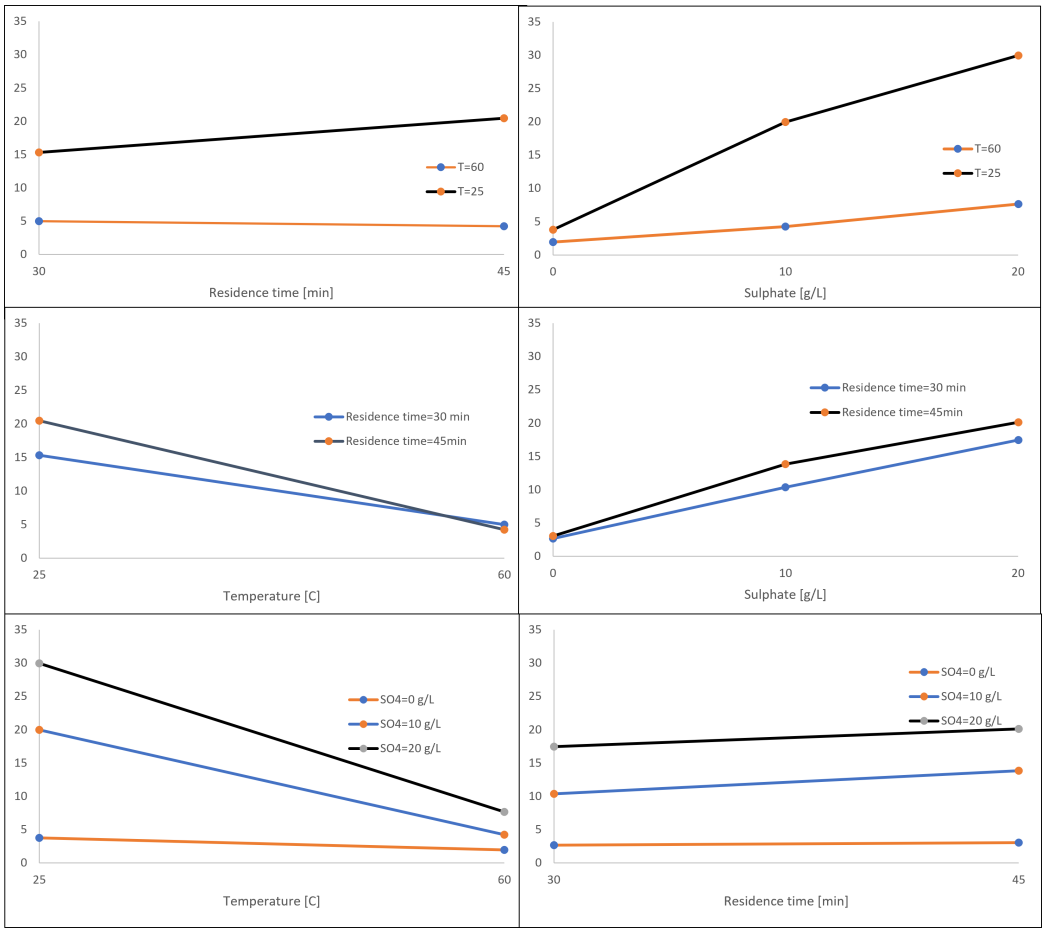


Figure 4.10: Top left and middle left: interaction plots for temperature and residence time. Top right and bottom left: interaction plots for temperature and sulphate concentration. Middle right and bottom right: interaction plots for residence time and sulphate concentration. For all of them the Y-axis is the amount of fluoride in the filtrate

## 4.3 Washing and Dissolving of Precipitate

Table 4.4 shows the result from the washing of the precipitate. Around 1 g of each of the precipitates, except $E_{25;45;0}$ and $E_{25;30;0}$ due to little precipitate, were weighed out. Three of the washing caused little of the precipitate to dissolve, the three corresponds to the ones without NaCl in Table 4.1. The washing should primarily remove the fluoride on the surface and the NaCl, due to it being easily dissolved, which is supported by the fact that the three that had no NaCl lost less mass. However, the amounts that have been dissolved are higher than the percentages of NaCl that had been estimated. The amounts of fluoride released are too insignificant, less than 1 mg, to account for this discrepancy between the weight loss and calculated NaCl. It also needs something to account for the loss for the samples without any NaCl. A likely possibility for the remaining weight is $Cl^-$-ions that have been adsorpted on the surface of the precipitate, and possibly some in the tunnels have been exchanged as well. Part of the discrepancy could also be caused by inaccurate estimates for NaCl by the Rietveld refinement.

The fluoride column is the total amount of fluoride that has been released into the de-ionized water. The amounts that were released is quite small compared to the initial amount of 100 mg/L. There is, however, an interesting difference between the experiments done at 25°C and with sulphate compared to the rest of the experiments, namely that they released more fluoride. This would indicate that $E_{25;30;10}$, $E_{25;30;20}$, $E_{25;45;10}$ and $E_{25;45;20}$ have more fluoride adsorpted on the surface of the precipitate compared to the rest. These were also the ones with the most fluoride left in the filtrate, thus it would be reasonable that they adsorped more, but this would be an indication that the other experiments precipitate with the fluoride as a part of the structure, in a way these four does not.

Table 4.5, 4.6 and 4.7 shows the results for the first, second and third dissolve respectively. After the first dissolve, there were no more $E_{25;45;0}$ and $E_{25;30;0}$, and after the second dissolve, there were no more $E_{60;30;0}$ and $E_{60;45;0}$ to continue to dissolve. The reason these ran out was twofold, for the first two, it was partly due to there being less to begin with, and secondly due to the precipitate and paper become inseparable. The precipitate without any sulphate present had large enough crystals to be filtered by the filter paper, but small enough to enter the pores of the filter paper, thus becoming difficult to separate. For example, sample $E_{60;30;0}$ had almost 0.6 g left after the first dissolving, but only 0.1168 g were possible to scrape off to use in the next part. The experiments with sulphate, on the other hand, were far easier to scrape off and therefore less solid were lost between each run. Looking at the lattice parameters of akaganeite from Figure 2.2 and the parameter for schwertmannite from Matteo Sestu(2015)[21], the largest difference is in the b-axis, where akaganeite is 3.03, while schwertmannite is 6.0622 Å, the parameters yield an approximate volume of the unit cell of 337 and 675 $Å^3$ for akaganeite and schwertmannite respectively. The larger

Table 4.4: Washing of the Precipitate

| | Solid weighed out [g] | Solid dissolved [g] | Fluoride [mg] |
|---|---|---|---|
| $E_{60;30;0}$ | 1.0071 | 0.1655 | 0.024562 |
| $E_{60;30;10}$ | 1.0273 | 0.1921 | 0.042447 |
| $E_{60;30;20}$ | 1.0094 | 0.1216 | 0.042620 |
| $E_{60;45;0}$ | 1.0090 | 0.0639 | 0.023491 |
| $E_{60;45;10}$ | 1.0164 | 0.1834 | 0.024562 |
| $E_{60;45;20}$ | 1.0016 | 0.1367 | 0.043669 |
| $E_{25;30;0}$ | 0.6325 | 0.2259 | 0.019575 |
| $E_{25;30;10}$ | 1.0317 | 0.2377 | 0.136923 |
| $E_{25;30;20}$ | 1.0080 | 0.0272 | 0.160366 |
| $E_{25;45;0}$ | 0.7872 | 0.1550 | 0.057291 |
| $E_{25;45;10}$ | 1.0036 | 0.1769 | 0.218207 |
| $E_{25;45;20}$ | 1.0130 | 0.0099 | 0.129896 |

crystals of schwertmannite might be too large to enter the pores of the filter paper and form a layer that prevents other smaller crystals from becoming stuck in it and therefore being the reason for the smaller discrepancy between the final weight after each dissolving and the starting weight for the next one.

The amount of fluoride that is released into the nitric acid is higher than the amounts that were released during the washing. This might be due to there being fluoride inside of the tunnels that gets released when the crystals get partially dissolved, but also might be caused by the surface area decreasing. If there had been a constant amount of fluoride that had been released compared to the amount of precipitate dissolved, it would have indicated that the fluoride was located inside of the tunnels, but in these experiments, the fluoride released varies. This variation would indicate that there is some fluoride adsorped on the surface of the precipitate, although the precipitate is a mix of different phases that might now be dissolved at a consistent ratio, and therefore cause this variation.

When all the fluoride measurements are added up, it only adds up to around 1-3 mg/g of the precipitate. The total amount of precipitation varied between 8-14g/L, thus the amount of fluoride on the solid varies between 8-42mg/L. However, in Table 4.3 the amount left in the filtrate went from 1.59 mg/l to 33.43 mg/L, meaning that the total amount adds up to significantly less than the 100 mg/L that were added to the reactor, even if adding the $\pm 10\%$ based on the nickel measurements. Because of the high variation and clear trends in the filtrate concentration, it would seem

Table 4.5: First Dissolving of Precipitate

| T[°C] | $\tau$ [min] | $SO_4$ [g/L] | Solid weighed out [g] | Solid dissolved [g] | Fluoride [mg] |
|---|---|---|---|---|---|
| 60 | 30 | 0 | 0.7530 | 0.1750 | 0.242530 |
| 60 | 30 | 10 | 0.7867 | 0.1746 | 0.484817 |
| 60 | 30 | 20 | 0.7490 | 0.2447 | 0.224486 |
| 60 | 45 | 0 | 0.8635 | 0.1479 | 0.219983 |
| 60 | 45 | 10 | 0.8212 | 0.2311 | 0.233770 |
| 60 | 45 | 20 | 0.7810 | 0.1523 | 0.403999 |
| 25 | 30 | 0 | 0.2916 | 0.1186 | 0.122236 |
| 25 | 30 | 10 | 0.8035 | 0.1840 | 0.195592 |
| 25 | 30 | 20 | 0.9731 | 0.1600 | 0.282817 |
| 25 | 45 | 0 | 0.5337 | 0.1791 | 0.140293 |
| 25 | 45 | 10 | 0.7857 | 0.1838 | 0.335292 |
| 25 | 45 | 20 | 0.9950 | 0.1762 | 0.328567 |

Table 4.6: Second Dissolving of Precipitate

| T[°C] | $\tau$ [min] | $SO_4$ [g/L] | Solid weighed out [g] | Solid dissolved [g] | Fluoride [mg] |
|---|---|---|---|---|---|
| 60 | 30 | 0 | 0.1168 | 0.0827 | 0.046783 |
| 60 | 30 | 10 | 0.5462 | 0.1367 | 0.202857 |
| 60 | 30 | 20 | 0.4858 | 0.1106 | 0.339393 |
| 60 | 45 | 0 | 0.1465 | 0.0897 | 0.067921 |
| 60 | 45 | 10 | 0.5435 | 0.1304 | 0.194801 |
| 60 | 45 | 20 | 0.5742 | 0.1104 | 0.194013 |
| 25 | 30 | 0 | - | - | - |
| 25 | 30 | 10 | 0.5760 | 0.1807 | 0.109567 |
| 25 | 30 | 20 | 0.7372 | 0.1694 | 0.139725 |
| 25 | 45 | 0 | - | - | - |
| 25 | 45 | 10 | 0.5370 | 0.1746 | 0.161672 |
| 25 | 45 | 20 | 0.7905 | 0.1877 | 0.136923 |

probable that all of the experiments had a significant amount of fluoride entering the reactor, which begs the question of where it has gone. The trends and amounts of fluoride in some of the filtrates, would indicate that this part is fairly accurate, while the extremely low amounts of fluoride in the dissolving part, compared to the differences in concentration of fluoride in the filtrate, indicates that the problem lay in the measurements of the dissolved precipitate. It is possible that the amounts

Table 4.7: Third Dissolving of Precipitate

| T[°C] | $\tau$ [min] | $SO_4$ [g/L] | Solid weighed out [g] | Solid dissolved [g] | Fluoride [mg] |
|---|---|---|---|---|---|
| 60 | 30 | 0 | - | - | - |
| 60 | 30 | 10 | 0.3743 | 0.1363 | 0.232824 |
| 60 | 30 | 20 | 0.3326 | 0.1140 | 0.467454 |
| 60 | 45 | 0 | - | - | - |
| 60 | 45 | 10 | 0.3485 | 0.1637 | 0.214699 |
| 60 | 45 | 20 | 0.3926 | 0.1412 | 0.196386 |
| 25 | 30 | 0 | - | - | - |
| 25 | 30 | 10 | 0.3371 | 0.1363 | 0.152137 |
| 25 | 30 | 20 | 0.5155 | 0.1835 | 0.152755 |
| 25 | 45 | 0 | - | - | - |
| 25 | 45 | 10 | 0.2883 | 0.1318 | 0.209541 |
| 25 | 45 | 20 | 0.5387 | 0.1652 | 0.147882 |

of iron in the dissolved part caused problems for the fluoride measurements, by the formation of iron-fluoride complexes, although the TISAB is supposed to prevent this and make the fluoride in the solution be present in ion form. Another possible explanation is the loss of solids between each dissolving caused by some of the precipitate getting stuck in the pores of the filter paper. It is possible that the precipitate lost adsorped the fluoride, causing the fluoride to leave the experiments this way. To identify the location of the fluoride in the precipitate more work is required, in particular more work on the dissolving of the precipitate.

# 5 Conclusions and Recommendations

This thesis has focused on the characterization of the precipitate, the fluoride removed by the filtration, and how sulphate concentrations, temperature and residence time have affected this.

The characterization of the precipitate showed that without any sulphate present most of the crystalline precipitate were akaganeite. When the amount of sulphate increased, the percentage of akaganeite and the crystallinity of the precipitate decreased. None of the experiments saw any significant decrease in the nickel amount in the filtrate, meaning that there was little loss of nickel to the precipitate, regardless of conditions.

The removal of fluoride was significantly affected by the amount of sulphate and the temperature. The remaining fluoride concentration went from 1.59 mg/L at the lowest to 33.43 t the highest. The experiments showed that the best fluoride removal were at a temperature of 60°C, sulphate concentration at 0 g/L and the residence time at 45 min. The main effect plot and interaction plot showed that there were significant interactions between the temperature and sulphate concentration.

The attempts to determine if the fluoride were located inside of the tunnels or not were inconclusive. There were some indications that the fluoride were located inside of the tunnels, but too little to state it with any certainty.

Future work should look more into the location of the fluoride as this work has only found some indications of its presence in the tunnels. One thing of significant interest was the filtration speed of the experiments. The experiments with sulphate filtered significantly faster than the ones without any sulphate present. A last thing that would be of interest for future work would be to separate the effect of nickel and chloride, to determine if the effect in these experiments is due to the sulphate, nickel or both.

# References


(1) Haynes, W. M., *ABUNDANCE OF ELEMENTS IN THE EARTH'S CRUST AND IN THE SEA, CRC Handbook of Chemistry and Physics*, 97th ed.; CRC: 2016–2017.

(2) WHO Fluoride in Drinking-water Background document for development of WHO Guidelines for Drinking-water Quality.

(3) Authority, E. F. S. TOLERABLE UPPER INTAKE LEVELS FOR VITAMINS AND MINERALS.

(4) Parsonage, D.; Singh, P.; Nikoloski, A. *Mineral Processing and Extractive Metallurgy Review - MINER PROCESS EXTR METALL REV* **2012**, *35*, DOI: 10.1080/08827508.2012.695306.

(5) Suarez, D.; Pinna, E.; Rosales, G.; Rodriguez, M. *Minerals* **2017**, *7*, DOI: 10.3390/min7050081.

(6) Zheng, Y.; Song, W.; Mo, W.-t.; Zhou, L.; Liu, J.-W. *RSC Adv.* **2018**, *8*, 8990–8998.

(7) Atia, D.; Hoggui, A. *Journal of Fundamental and Applied Sciences* **2015**, *5*, 129.

(8) Ghorai, S.; Pant, K. *Separation and Purification Technology* **2005**, *42*, 265–271.

(9) Samatya, S.; Yüksel, Ü.; Yüksel, M.; Kabay, N. *Separation Science and Technology* **2007**, *42*, 2033–2047.

(10) Kuang, L.; Liu, Y.; Fu, D.; Zhao, Y. *Journal of Colloid and Interface Science* **2017**, *490*, 259–269.

(11) Kumar, E.; Bhatnagar, A.; Ji, M.; Jung, W.; Lee, S.-H.; Kim, S.-J.; Lee, G.; Song, H.; Choi, J.-Y.; Yang, J.-S.; Jeon, B.-H. *Water Research* **2009**, *43*, 490–498.

(12) Tang, Y.; Guan, X.; Wang, J.; Gao, N.; McPhail, M. R.; Chusuei, C. C. *Journal of Hazardous Materials* **2009**, *171*, 774–779.

(13) Pepper, R. A.; Couperthwaite, S. J.; Millar, G. J. *Journal of Environmental Chemical Engineering* **2018**, *6*, 2063–2074.

(14) Peretyazhko, T.; Pan, M.; Ming, D.; Rampe, E.; Morris, R.; Agresti, D. *ACS Earth and Space Chemistry* **2019**, *3*, DOI: 10.1021/acsearthspacechem.8b00173.

(15) Cai, J.; Liu, J.; Gao, Z.; Navrotsky, A.; Suib, S. L. *Chemistry of Materials* **2001**, *13*, 4595–4602.

(16) Peretyazhko, T.; Fox, A.; Sutter, B.; Niles, P.; Adams, M.; Morris, R.; Ming, D. *Geochimica et Cosmochimica Acta* **2016**, *188*, 284–296.

(17) Peretyazhko, T.; Ming, D.; Rampe, E.; Morris, R.; Agresti, D. *Journal of Geophysical Research: Planets* **2018**, *123*, DOI: 10.1029/2018JE005630.

(18) Ståhl, K.; Nielsen, K.; Jiang, J.; Lebech, B.; Hanson, J.; Norby, P.; Lanschot, J. *Corrosion Science* **2003**, *45*, 2563–2575.

(19) Shannon, R. *Acta Crystallographica Section A* **1976**, *32*, 751–767.

(20) Mullin, J. In *Crystallization (Fourth Edition)*, Mullin, J., Ed., Fourth Edition; Butterworth-Heinemann: Oxford, 2001, pp 315–402.

(21) Sestu, M. The structure of nano sized poorly-crystalline ironoxy-hydroxides, 2015.

# A Data

Url:https://1drv.ms/x/s!Aisfa6Jj5ra2htIeW7ldt40fAeMR2A?e=wrLwe2

Following is an example equation to calculate the concentration of fluoride given a measured mV of 137.7:

$$c_f = 2 * 10^{\frac{137.7-115.66}{-56.82}}$$